CHAPTER 2

Materials and Methods

2.1 Introduction

This chapter is devoted to the description of the experimental procedure followed for the synthesis of g-C_3N_4/NiO, Ag/NiO and NiS/ZnO nanocomposites. Moreover, the photocatalytic performance of as synthesized photocatalysts was evaluated by the degradation of malachite green (MG), rhodamine B (RhB), and p-nitrophenol (PNP) under UV light irradiation. This chapter also deals with the working principle of different instrument utilized to characterize the synthesized nanocomposites.

2.2 Materials

All the chemicals utilized for the synthesis of nanocomposite photocatalysts (g-C_3N_4/NiO, Ag/NiO, and NiS/ZnO) were of analytical grade (AR) and used as obtained without further purification. Table 2.1 contains the details of the chemicals used during the synthesis.

Table 2.1 Details of the chemicals used in the thesis

Sr. No.	Chemical name	Chemical formula	Molecular weight (g)	Manufacturer	Physical Appearance
1	Nickel nitrate hexahydrate	$Ni(NO_3)_2.6H_2O$	290.81	Sigma aldrich	Green Crystal
2	sodium citrate tribasic dihydrate	$C_6H_5Na_3O_7.2H_2O$	294.10	Merck	White powder
3	Ethyl alcohol	C_2H_5OH	46.00	Merk	Colorless liquid
4	Melamine	$C_3N_3H_6$	126.12	Alfa aesar	White powder
5	Malachite green	$C_{23}H_{25}ClN_2$	364.91	Sigma aldrich	Bluish-green
6	Silver nitrate	$AgNO_3$	169.87	Sigma aldrich	White Crystal
7	Sodium hydroxide	NaOH	40.00	Merck	White Pellet
8	Citric acid	$C_6H_8O_7$	192.12	Merk	White

					powder
9	Sodium borohydride	$NaBH_4$	37.83	Sigma aldrich	White Crystal
10	Rhodamine B	$C_{28}H_{31}ClN_2O_3$	479.02	Merk	Reddish-violet
11	Zinc nitrate hexahydrate	$Zn(NO_3)_2.6H_2O$	297.50	Sigma aldrich	White Crystal
12	Thiourea	CH_4N_2S	76.12	Merk	White powder
13	para-nitrophenol	$C_6H_5NO_3$	139.11	Merk	Pale yellow crystal
14	para benzoquinone	$C_6H_4O_2$	108.09	Merck	Yellow Crystal
15	isopropyl alcohol	C_3H_8O	60.10	Merk	Colorless liquid
16	Potassium iodide	KI	166.00	SRL	White crystal

2.3 Sample preparation

All the materials of this thesis were synthesized either by hydrothermal or by sol-gel methods, for the hydrothermal synthesis a Teflon lined stainless steel autoclave were used as a reaction vessel. The details about the materials synthesis is discussed in the experimental sections of respective chapters 3, 4 and 5.

2.4 Characterization Techniques

2.4.1 High resolution X-ray diffraction pattern (HR-XRD)

The HR-XRD patterns of the synthesized photocatalysts were carried out through Rigaku smartLab 9kw instrument to determine the structural properties (lattice parameter, grain size, phase composition) crystallinity, and crystal phase of the material. This instrument consists of photon max high flux 9kw X-ray source, closed loop goniometer, optics and silicon strip detector. The used tube voltage and tube current of the instrument was set in the range of 20-45 kV and 10-200 mA respectively. The instrument works with Cu-Kα radiation having a

wavelength (λ = 1.54059 Å); figure 2.1 presents a picture of typical HR-XRD instrument.

Fig. 2.1 HR-XRD instrument

Principle of XRD

In XRD technique the Diffraction of X–rays is based on the constructive interference between X-rays (monochromatic) generated by a cathode tube and crystalline samples. Constructive interference produced by the interaction of monochromatic X-rays of λ wavelength with the materials and the diffracted rays were formed if condition satisfies the Bragg's equation (figure 2.2 represents the Bragg's diffraction)

$$(\boldsymbol{n\lambda = 2dsin\theta}) \qquad (\mathbf{2.1})$$

Where,

n = order of diffraction (n = 1, 2, 3,…..etc.);

λ = wavelength of X-rays;

d = interplaner distance between two adjacent planes;

θ = Bragg angle or angle of diffraction;

further the formed diffracted X-rays were detected by silicon strip detector and signals are processed, converted and sent to an output device which displays the peaks, X-ray diffractometer follows two types of geometry based on the movement of source, sample and detector; i.e. θ — θ and θ — 2θ geometry. In θ — θ geometry source and detector rotates while sample kept constant, whereas in case of θ — 2θ sample and detector rotates while source kept constant. The obtained XRD data then matched with the standard data published by International Center for Diffraction Data (ICDD).

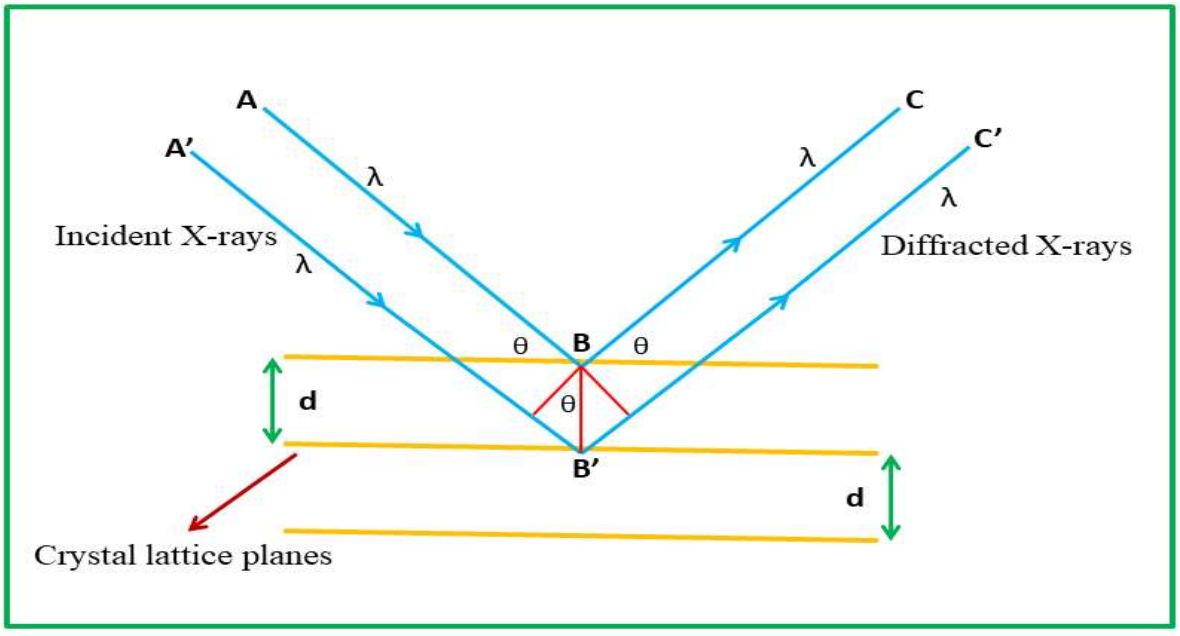

Fig. 2.2 Schematic representation of Bragg's diffraction

Furthermore, the average crystallite size can be calculated with the help of the Scherrer equation

$$D = \frac{k\lambda}{\beta cos\theta} \qquad (2.2)$$

Here, D simply denotes the average crystallite size (nm), k represents a dimensionless shape

factor (≈0.9), λ is the wavelength of X-ray (1.542 Å), β signifies the full width at half maximum (FWHM) intensity in radians while, θ is the Bragg angle.

2.4.2 Fourier Transform Infrared Spectroscopy (FT-IR)

The Fourier Transform Infrared (FT-IR) spectrum of the synthesized nanocomposites was recorded by Thermo electron scientific instrument (Nicolet iS5). The FTIR analysis of the synthesized nanocomposites was performed to know the types of vibration present in the sample. For FTIR, the sampling was done by KBr pellatization method and the FTIR spectra were recorded in the range of 400-4000 cm^{-1}.

Principle of FTIR

Fourier transform infrared spectroscopy (FTIR) is a characterization technique, mainly used to identify the chemical bonds present in compounds and types of vibration present in the molecule. FTIR spectroscopy is observed due to the interaction of infrared radiation with the materials, like other spectroscopic techniques it is also govern by some specific selection rule, i.e. only those materials will be IR active which possess change in dipole moment during the interaction. FTIR spectrometer mainly consists of three parts, i.e., a source, a sample holder and a detector. The beam of infrared (IR) radiations emitted by the source sent to interferometer where it is splitted into two parts by a beam splitter; first half of the beam is refracted from steady mirror while the other half is transmitted through moving mirror. Further the reflected lights from steady and movable mirror returns to the beam splitter and the difference between the paths of the two beams frame the constructive and destructive interference which is referred as interferogram, after that the lights passing through specimen compartment where it is absorbed at different wavelength and is collected by the detector which generates raw data belongs to the time domain. As with the help of some mathematical

formulas of Fourier transform, the obtained interferogram in time domain can be converted into frequency domain, that's why its name is Fourier transform infrared spectroscopy (FTIR).

2.4.3 Transmission Electron Microscopy (TEM)

Transmission Electron Microscopy (TEM) is a microscopic technique which has been used to visualize particles with highly resolved (magnified) images. TEM images of the synthesized samples were recorded on Tecnai G2 20 TWIN instrument (figure 2.3) with an accelerating voltage of 200 kV. In order to characterize the synthesized materials through TEM we have re-dispersed the prepared samples in 30 mL of water by ultrasonication for 40 minutes. Further 10-15 uL of the dispersed samples were deposited on a carbon coated copper grid and it was dried overnight in an oven at 75^0C after that this grid was placed in sample holder for microscopic studies.

Principle

TEM micrographs of the samples provide detailed information about the structure, crystallinity and phase of the specimen. Moreover, energy dispersive X-ray spectroscopy (EDS) gives the information about the elemental composition in a selected region of a sample. This technique uses high energy electron beam which interacts with the material then the beam scattered from the sample is responsible to create images.

TEM mainly have four segments; electron gun, condenser system, image producing segment (objective and projection lense) and image detecting system. The beam of electrons produced from electron gun is passes through condenser lenses to get required convergence angle. After that these highly energetic electrons interact with the matter and then pass through different lens system (objective, intermediate and projection lenses); these lenses focus on

electrons to produce true and highly resolved picture of the specimen. The modern TEM has about 0.2 nm resolution which is much higher (almost 1000 times) than the resolution of light microscope.

Fig. 2.3 Image of TEM instrument

2.4.4 Field Emission Scanning Electron Microscopy (FE-SEM)

FE-SEM is a microscopic technique that works with electrons which are generated by a field emission source. This technique is used to get the topographic picture of the surface of even very small particles (1 nm). In FE-SEM the electrons liberated from a field emission gun (FEG) and accelerated under the action of high electric field gradient these accelerated electrons called as primary electrons are focused and deflected by different types of lenses resulting to this the beam gets narrower; this narrow beam interacts with the specimen (matter) and due to this interaction secondary electrons are generated from each spots on the

specimen. The velocity and angle of the secondary electron depends on the surface structure of the materials under investigation. Further these secondary electrons are detected by a detector and produces electronic signals corresponding to them, these electronic signals are amplified and transformed in the form of scaned images which displays on monitor. An image of FE-SEM instrument (Model: Nova Nano SEM 450) is provided in figure 2.4.

Fig. 2.4 Image of FE-SEM instrument

2.4.5 X-ray Photo Electron Spectroscopy (XPS)

X-ray photoelectron spectroscopy (XPS) is a technique which is used to identify the elements present in a sample and their chemical states. This technique is based on the principle of photoelectric effect; it utilizes photo-ionization to measure the kinetic energy of the ejected electrons in order to determine the elemental composition and chemical state of the material. Figure 2.5 showing the instrumentation and working of a XPS instrument.

In XPS, when surface of the sample is bombarded by X-rays, the highly energetic X-rays having energy equal to hν may ionizes the atoms by knocking out core electrons from the valence shell (outermost shell). The energy difference of ionized and neutral species is known as binding energy of electron. The transition energy of the ejected electrons is balanced with the emission energy of X-rays (Auger electrons). Further these photo ejected electron and emitted Auger electrons are detected by a detector and converted it into a signal to represent the surface composition of the sample. In XPS peaks the area below the peak relatively measures the amount of the elements present. However, the peak positions determine the chemical states of the electrons in the material.

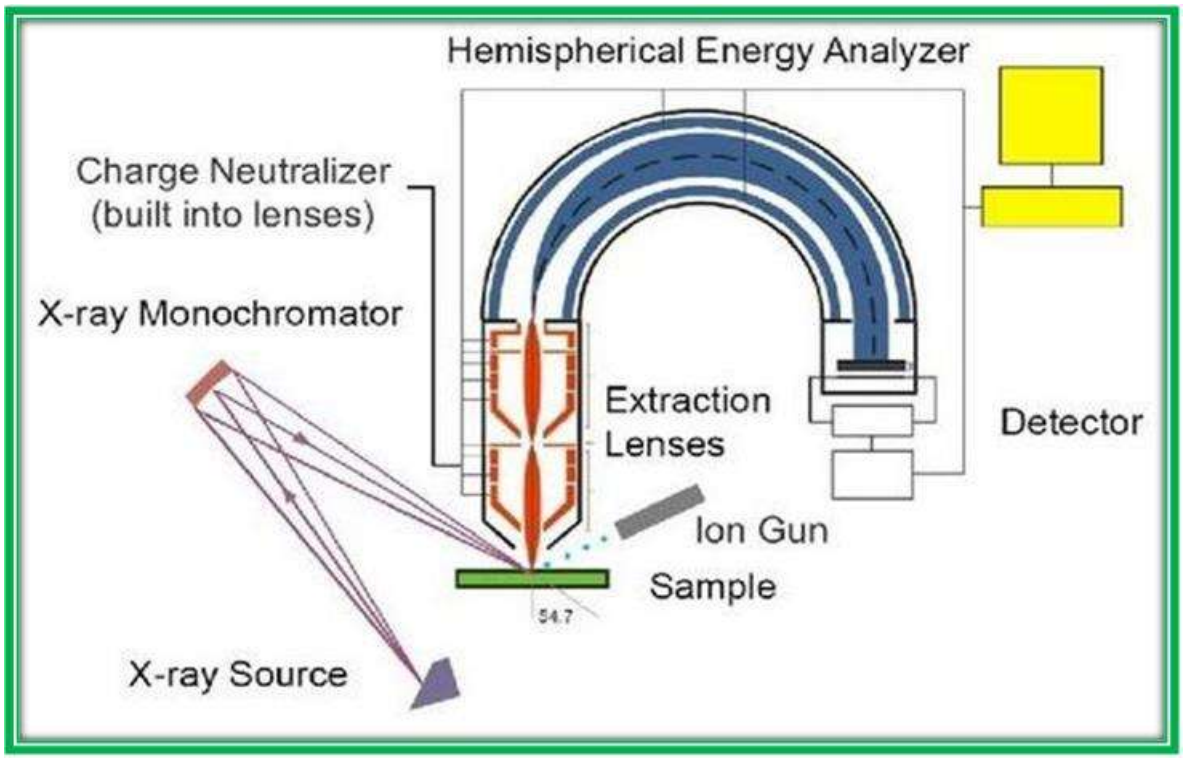

Fig. 2.5 Diagram showing instrumentation in XPS

[Image courtesy: (google.com xps instrumentation)]

2.4.6 N_2 Adsorption-Desorption Analysis

Determination of the specific surface area, pore size distribution and the surface texture of photocatalysts are very important in the field of photocatalysis as these factors plays crucial role towards their activity. The adsorption of nitrogen (at lower temperature) over the porous surface of the material is a most common method utilized for this purpose. This adsorption of nitrogen (N_2) on the material's surface is dictated in terms of the relative pressure $\left(\frac{P}{P_0}\right)$ of N_2. Here, *P* denotes the partial pressure of nitrogen and while P0 is the vapor pressure of N_2 at 77 K (temperature of liquid N_2). The range of relative pressure used for Brunauer, Emmett, and Teller (BET) equation is 0.05-0.35 (Fu et al., 2017).

BET equation given as follow

$$\frac{\boldsymbol{P}}{\boldsymbol{V(P_0 - P)}} = \frac{\boldsymbol{1}}{\boldsymbol{V_m C}} + \left(\frac{\boldsymbol{C-1}}{\boldsymbol{V_m C}}\right)\left(\frac{\boldsymbol{P}}{\boldsymbol{P_0}}\right) \qquad \boldsymbol{(2.3)}$$

Here, "V" represents volume of the gas adsorbed under pressure; "V_m" is the adsorbate's volume required for the monolayer coverage; "C" denotes the constant of heat of adsorption and liquefaction; "P_0" is the saturation vapor pressure of adsorbate and "P" is the adsorption pressure at equilibrium.

This principle is used for measuring the specific surface area by nitrogen physisorption method. If the value of $\left(\frac{P}{P_0}\right)$ is ≥ 0.40 then, the condensation of N_2 occurs in the micropores caused by capillary condensation. The distribution of pore size can be measured by analyzing N_2 adsorption-desorption isotherm. BET Isotherm is the most reliable and widely used technique in determining the specific surface area, pore dimensions and texture of the material. The concept of BET Isotherm is evolved from Langmuir's theory which deals with the monolayer adsorption.

Prior to the analysis, the material's is required to degas in order to remove the impurities physically bonded to the surface of the material. This degassing is done at elevated temperature with a continuous flow of inert gas. This process must be carefully monitored to get repeatable and accurate result. The surface area of the sample is measured by the physisorption of nitrogen gas onto the surface of the sample at liquid nitrogen temperature of 77K. The amount of gas adsorbed is directly related to the specific surface area of the sample. The physical adsorption corresponding to the monolayer of the surface of the sample is a result of weak Van-der Waals forces between the surface of the sample and gaseous molecules of the adsorbate.

2.4.7 UV-Visible Diffuse Reflectance Spectra (UV-Vis DRS) and Procedure to Determine the Band gap of the Material

UV-Vis DRS spectra were recorded by Shimadzu Pharmaspec UV-1700 instrument in the range of 200-800 nm to get the absorbance data which was used for calculation of the band gap of materials.

As the knowledge of actual band gap is essential to explain the photocatalytic mechanism, and this band gap was calculated by putting the absorbance data obtained from the UV-Vis. DRS in to given equation (2.4).

$$(\alpha h\nu)^{1/n} = \left(h\nu - E_g\right) \qquad (2.4)$$

Above equation is known as Tauc and Davis-Mott relation. This relation is used to probe the optical band gap energy of nanoparticles from UV-Visible absorption spectroscopy. In this equation "α" denotes the absorption coefficient "hν" is the energy of the incident photon, and Eg presents the optical band gap energy of the material. The exponent "n" in the equation represent the mode of transition. For direct transition n = ½ while for the indirect transition

the value of n will be 2. In tauc plot method, we plot energy (E_g) on x-axis while $(\alpha h\nu)^{1/n}$ on y-axis. Then draw the tangent line on the curve where $\alpha = 0$. The point where it touches the x-axis is the optical band gap energy of the material. UV-Visible spectroscopy only records the wavelength and absorbance data of the material. Therefore, it is required to convert wavelength to energy and calculate absorbance coefficient (α) from the absorbance data.

Here, Max Plank equation is used to calculate energy from the wavelength i.e.

$$E_g = h\nu \qquad (2.5)$$

Where h is plank constant and ν is the frequency of incident photon.

As we know that,

$$\nu = \frac{c}{\lambda} \qquad (2.6)$$

c is the speed of light, λ is the wavelength of incident photon.

Now, put the eq. (2.6) into equation (2.5)

$$E_g = \frac{hc}{\lambda} \qquad (2.7)$$

$h = 6.62 \times 10^{-34}$ js, $c = 2.99 \times 10^{8}$ m/s

After putting these values in equation (2.7) it will be

$$E_g = \frac{6.62 \times 10^{-34} \times 2.99 \times 10^{8}}{\lambda}$$

$$E_g = \frac{19.85 \times 10^{-26}}{\lambda} \qquad (2.8)$$

In equation (2.8), the energy is in joules, so, we have to convert it into electron volts.

As we know that,

$1 \text{ eV} = 1.602 \times 10^{-19}$ j

Therefore Energy in equation (2.8) can be converted as follow,

$$E_g = \frac{19.85 \times 10^{-26}\text{j m}}{1.602 \times 10^{-19} j \times \lambda}$$

$$E_g = \frac{12.39 \times 10^{-7}\text{eV m}}{\lambda}$$

$$E_g = \frac{1239.3 \times 10^{-9}\text{eV m}}{\lambda}$$

$$E_g = \frac{1239.3 \text{ eV nm}}{\lambda} \quad (\text{As, } 10^{-9} = \text{nano})$$

So,

$$E_g = \frac{1240 \text{ eV nm}}{\lambda} \qquad (2.9)$$

In equation (2.9) if λ is in nanometer (nm), then we get energy in eV

Now, on y-axis we will have $(\alpha h\nu)^{1/n}$.

Here hν is the incident photonic energy and α is the absorbance coefficient. We can calculate α from absorbance data by using Beer - Lambert's law.

$$\frac{I}{I_0} = e^{-\alpha l} \qquad (2.10)$$

Here, "I" is the intensity of transmitted light, "I_0" is the intensity of incident light, "α" is the absorbance coefficient and "l" is the path length of light in which absorbance take place.

Taking log on both side of equation (2.10) we get

$$log\left(\frac{I}{I_0}\right) = log\,(e^{-\alpha l})$$

$$log\left(\frac{I}{I_0}\right) = -\alpha l\, log\,(e)$$

$$-log\left(\frac{I}{I_0}\right) = \alpha l\, log\,(e)$$

$$log\left(\frac{I_0}{I}\right) = \alpha l\, log\,(e) \qquad (2.11)$$

As, Absorbance (A) = $\boldsymbol{log}\left(\frac{I_0}{I}\right)$

Hence, equation (2.11) can also be written as,

$$\boldsymbol{A = \alpha l \log (e)}$$

Or

$$\boldsymbol{\alpha = A\frac{1}{\log (e) l}}$$

Since, $\log (e)$ = 0.4343

So,

$$\boldsymbol{\alpha = A\frac{1}{0.4343\, l}}$$

$$\boldsymbol{\alpha = 2.303 \times \frac{A}{l}} \qquad \boldsymbol{(2.12)}$$

In standard cuvettes the path is usually equal to 10 mm, i.e. l = 10 mm = 1 cm

Therefore, equation (2.12) can be written as

$$\boldsymbol{\alpha = 2.303 \times \frac{A}{1\, cm}} \qquad \boldsymbol{(2.13)}$$

Or

$$\boldsymbol{\alpha = 2.303 \times A\,(cm^{-1})} \qquad \boldsymbol{(2.14)}$$

Now, equation (2.14) is combined with energy to get Tauc relation i.e.

$$\boldsymbol{(\alpha h\nu)^{\frac{1}{n}} = (Absorbance\ coefficient \times Energy)^{\frac{1}{n}}}$$

$$\boldsymbol{(\alpha h\nu)^{\frac{1}{n}} = (2.303 \times A \times h\nu)^{\frac{1}{n}}}$$

Figure 2.6 displays the Tauc plot of a sample for the direct transition (i.e. n = ½).

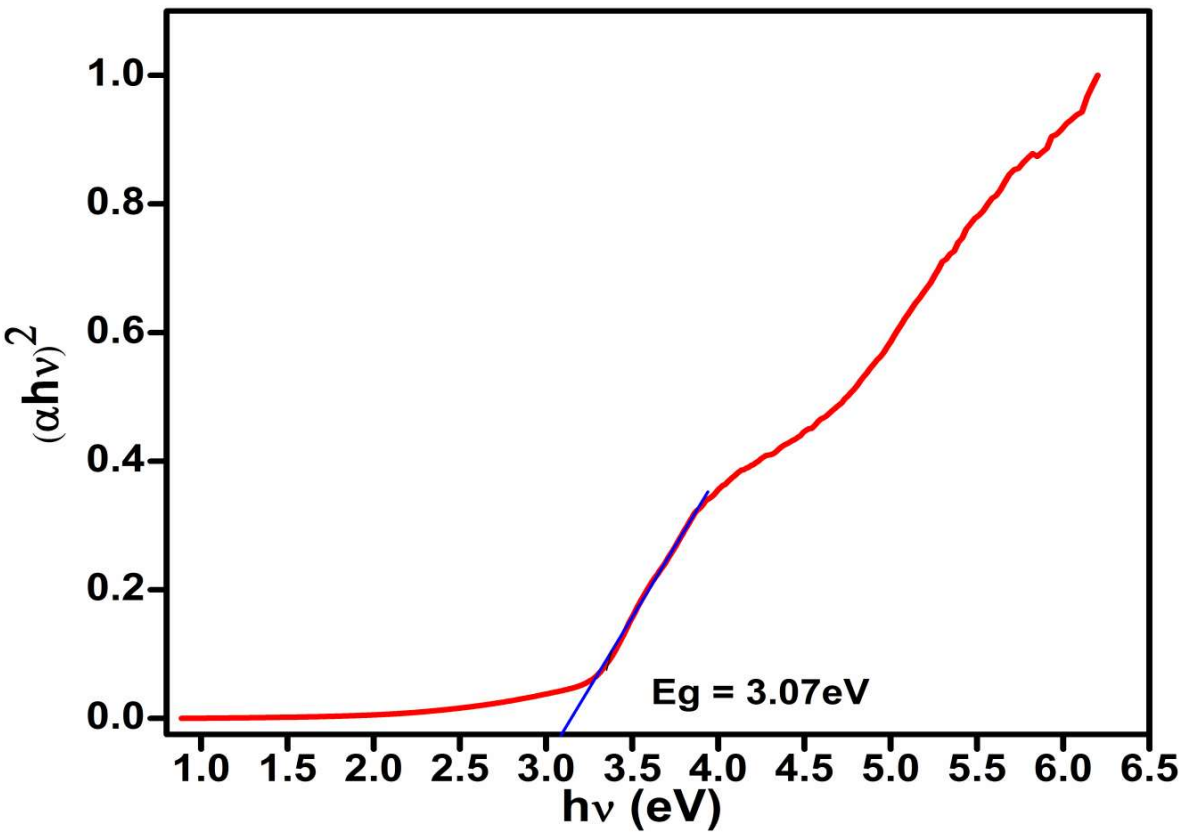

Fig. 2.6 Tauc plot of a sample

2.4.8 UV-Visible Spectroscopy

Ultraviolet–Visible (UV-Vis) spectroscopy is a technique that is used to measure the amount of discrete wavelength of light (UV or Visible), it is an absorption spectroscopy and uses electromagnetic radiation in the wavelength range of 200-800 nm (200-400 nm UV region and 400-800 nm visible region), when electromagnetic radiation having wavelength falls in this range interacts with the sample various types of transitions may occur in the molecules such as, σ-σ*, σ-π*, π-π*, n-π* and n-σ* (figure 2.7).

The working principle of UV-Vis spectroscopy is based on Beer-Lambert's law. According to Lambert's law absorbance of light by a medium does not depends on the intensity of the incident light but it is directly proportional to the path length of the cuvette or we can say thickness of the material. However, Beer's law states that absorbance of light is directly

proportional to the concentration of the solution.

Following equation is the mathematical expression of the Beer-Lambert's law

$$A = log\frac{I_0}{I} = \varepsilon cl \qquad (2.15)$$

Here I_0 and I denotes the intensities of the incident and transmitted light respectively, A signifies the absorbance, ε represents the molar absorptivity (molar extinction coefficient), c is the molar concentration of solute in solution and l denotes the path length of the cuvette.

Figure 2.8 displays the schematic representation of working of UV-Vis spectrophotometer, from the figure it can be seen that the light, which comes from the source (deuterium lamp is used for UV light source while tungsten lamp is for visible light) passes via filter and monochromator, after that the monochromatic beams gets splits into two beams by a beam

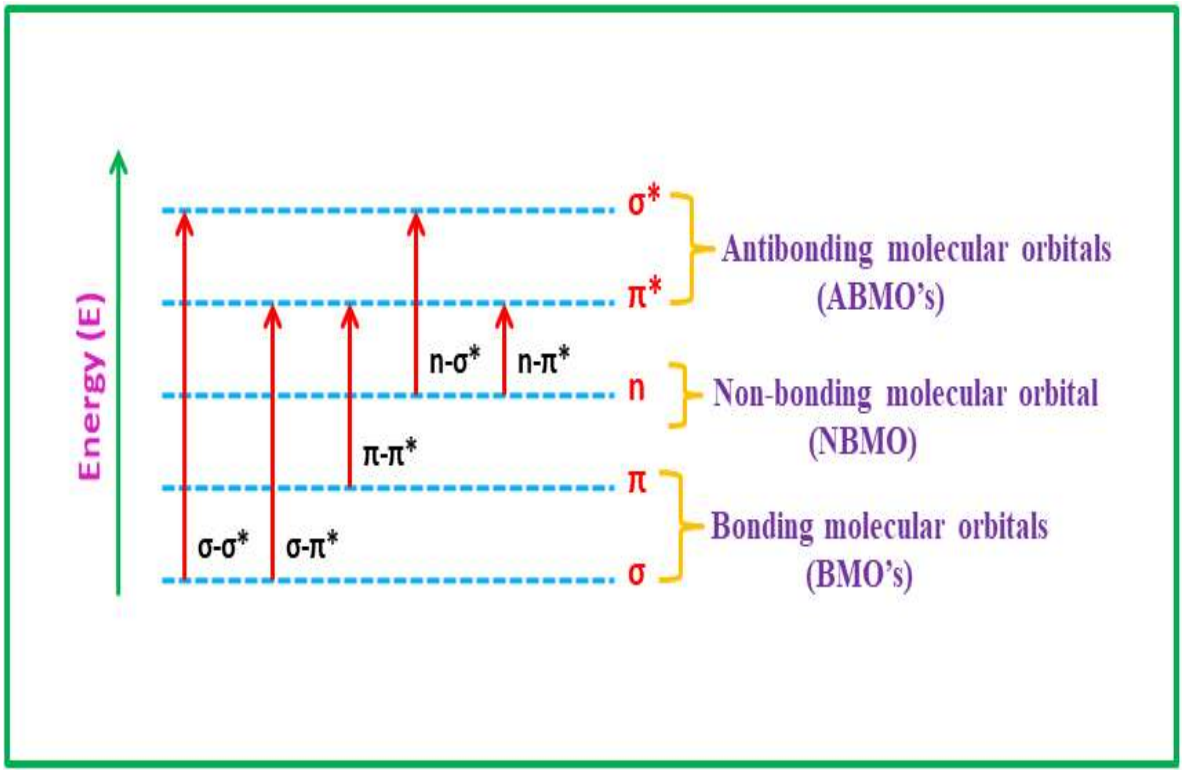

Fig. 2.7 Possible electronic transitions when lights interact with matters

Splitter and these splitted beams pass through the cuvettes of the sample solution and

reference solution separately, and then both the beams come out from the cuvettes and travels to the photodiode, where the relative intensity of both the beams recorded and compared. The beam coming through the reference solution is referred as I_0 (because there is no absorption of light) whereas; the same coming from sample solution is referred as I.

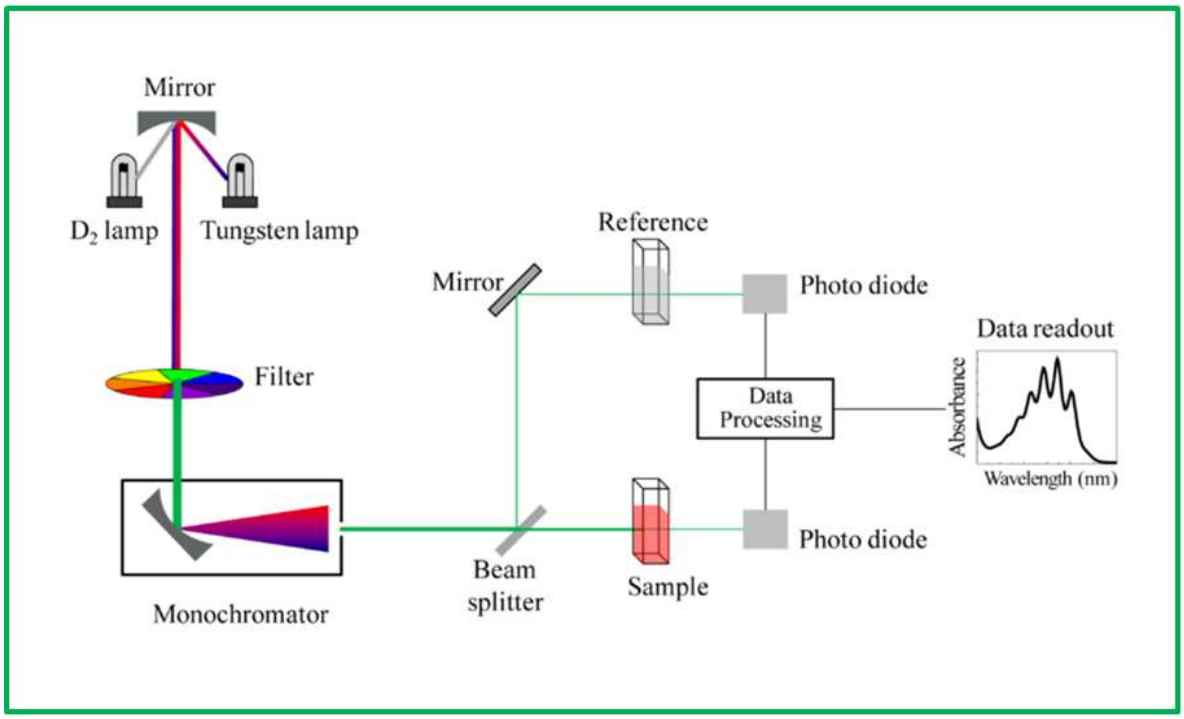

Fig. 2.8 Schematic representation of working of double beam UV-Vis spectrophotometer [image courtesy: Wikipedia (https://www.wikipedia.org/)]

2.4.9 Photoluminescence (PL) spectroscopy

Simply the term luminescence refers to the phenomenon of absorption of photons of electromagnetic radiation by matter followed by consequential light emission. If light is used as source of excitation then it is called as photoluminescence. The instrument used to record the photoluminescence (PL) spectra is known as spectrofluorometer. This spectrofluorometer has two spectrometer; one is exciting spectrometer and another one is analyzing spectrometer. The working principle of PL spectroscopy is very simple, when photons of

light absorbed by the matter then the electrons gets transit into higher excited states, and when these excited electrons returns back to their normal states they release some energy either via radiative or via non-radiative process. Figure 2.9 displays the famous Jablonski diagram, which represents all the possible transitions may occurs during photoluminescence.

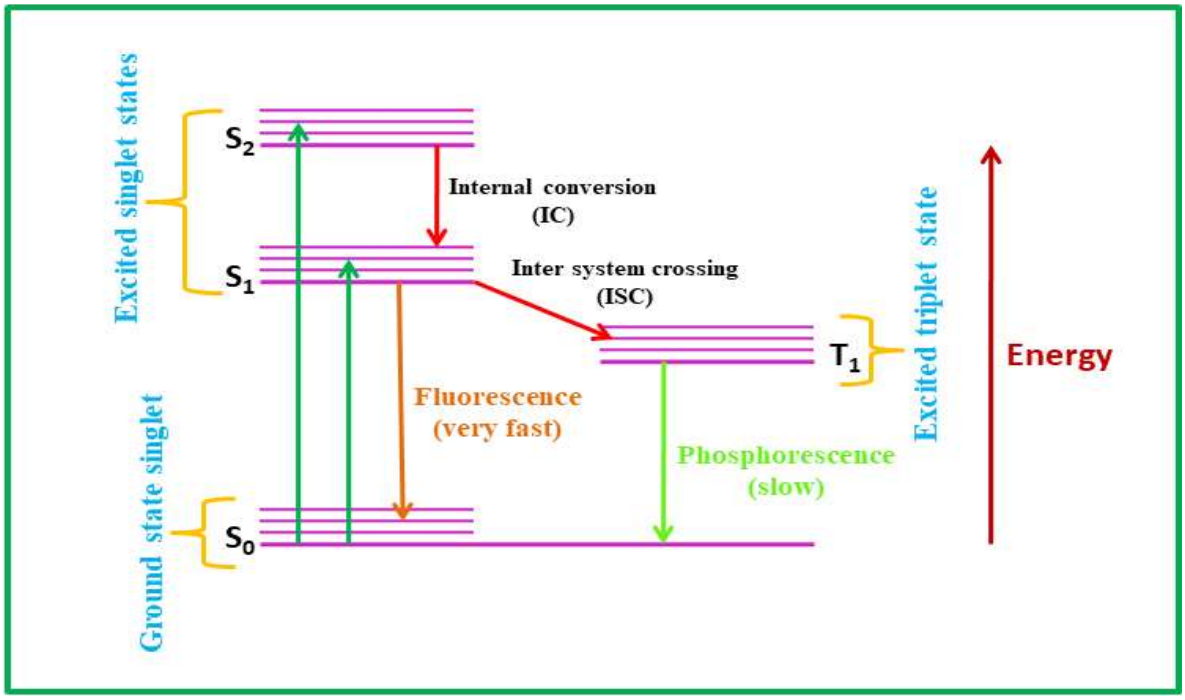

Fig. 2.9 Jablonski diagram (Energy diagram) for photoluminescent system

There is mainly two types of luminescence i.e. Fluorescence and phosphorescence. In case of fluorescence the emission takes place from first excited singlet to ground state. Fluorescence is a spontaneous process and it occurs in between 10^{-9}–10^{-7} seconds. So, it takes place as long as source of excitation is provided and when this source is removed the phenomenon of fluorescence gets stop. Moreover, phosphorescence is just like fluorescence but in case of former the emission occurs from triplet state to the ground state it is a slow process (10^{-3}-10^{0} seconds), hence phosphorescence can occur even after source of excitation gets removed.